2009

Feedback Sensor Development for IR-Based Heaters Used in Animal Housing Micro-Climate Control

Steven J. Hoff
Iowa State University, hoffer@iastate.edu

FEEDBACK SENSOR DEVELOPMENT FOR IR-BASED HEATERS USED IN ANIMAL HOUSING MICRO-CLIMATE CONTROL

S.J. Hoff

ABSTRACT. *The development of a feedback control sensor for flame-based infrared (IR) heaters used in animal agriculture is described. The intended use of this sensor is to control the heating pattern at desired levels for young animals in enclosed housing applications to desired micro-climate specifications. The sensor developed was sensitive to placement position in the IR heat pattern but once a suitable location was found, representative heating temperatures in the heating pattern were described very well. The first-ordered behaving IR sensor developed had a heat-up time constant of 7.5 min and a cool-down time constant of 9.5 min. The IR sensor was demonstrated in a closed-loop control scenario where the controlled IR heating zone was maintained within ±1.2 ℃ (±2.2 ℉) using a three-stage gas modulating control system.*

Keywords. *Infrared, Sensor, Micro-climate, Control, Heating.*

Using infrared (IR) heating to control the micro-climate for young animals is a common practice. However, little is known regarding IR-based heating patterns and the corresponding thermal environment developed in the animal occupied zone (AOZ). As energy conservation measures become a top priority, methods are needed that provide the best AOZ climate at the lowest possible energy input. One method is to first sense the thermal conditions in the AOZ and control these conditions at desired levels, using lower energy input, provided feedback sensing techniques exist to provide this function. In terms of IR-based micro-climate control, little is known about sensing the AOZ conditions as affected by IR-heating and the relationship between feedback sensing location, feedback sensor design, and the actual thermal conditions experienced in the AOZ. If an accurate IR sensor could be developed, control strategies could then be developed to minimize energy input to IR-based heaters while maintaining the AOZ at desired thermal conditions. This research project was specifically designed to develop and evaluate an IR sensor to be used for controlling the micro-climate at desired conditions using flame-based IR heaters.

LITERATURE REVIEW

CHARACTERISTICS OF RADIANT HEAT

Infrared (IR) radiation can be divided into five characteristic wavelength ranges (Miller, 1994) consisting of near-infrared (NIR; $0.75<\lambda<1.1$ μm), short-wavelength infrared radiation (SWIR; $1.1<\lambda<3$ μm), mid-wavelength infrared radiation (MWIR; $3<\lambda<6$ μm), long-wavelength infrared (LWIR; $6<\lambda<18$ μm), and far-infrared (FIR; $18<\lambda<1000$ μm). Infrared radiation has both a spectral and directional dependence and generally depends upon a number of factors such as the temperature of the emitting source, emissivity (ε) of the source surface, and radiation path length determined by the geometry between source and receiver (Hall, 1962; Modest, 1993; Holman, 2002).

The wavelength of maximum emission from an infrared source is a function of temperature according to Wien's Displacement Law (Holman, 2002). The emission properties of the heating source and the absorption properties of a receiver are dependent upon this wavelength. The production of IR energy is usually achieved with electrical filaments or flames; both of which are commonly used in animal housing micro-climate control. For flame-based IR heaters, liquid propane (LP) is the most common fuel source. The theoretical maximum flame temperature for propane with air as the oxidant, assuming perfect stoichiometric combustion, is 2253 K (Barnard and Bradley, 1985). Based on Wien's Displacement Law ($\lambda_{max}T=2897$ μm-K; Holman, 2002), the maximum radiant energy would be emitted at 1.29 μm implying that an LP-based IR heater emits in the NIR to SWIR spectrums.

IR energy that is emitted from a flame-based source will be reduced by imperfections in transferring combustion energy to a thermal emitter of a given temperature and absorption in the airspace between the source and the receiver with the receiver affected as well by the geometry between the source and receiver.

RADIANT HEAT USE IN ANIMAL AGRICULTURE

Zhou and Xin (2001) studied radiant heat lamp use in farrowing micro-climates investigating the differencing in performance and energy use with constant and variable output lamps. They showed no significant differences in average daily gain or heat lamp use based on pig behavior for the two strategies but did show significant energy savings with variable output lamp use. Zhang and Xin (2001) investigated piglet preferences between heat lamps and heat mats in the creep area of a farrowing crate and found that

Submitted for review in December 2008 as manuscript number SE 7842; approved for publication by the Structures & Environment Division of ASABE in March 2009.

The author is **Steven J. Hoff, ASABE Member Engineer,** Professor, Department of Agricultural and Biosystems Engineering, 212 Davidson Hall, Iowa State University, Ames, Iowa 50011; phone: 515-294-6180; fax: 515-294-2255; e-mail: hoffer@iastate.edu.

piglets preferred heat lamp use over heat mats for the first two days after birth and reported that for heat lamps, a linear decrease in piglet surface temperature was found with increasing radial distances from the heat source center-line. Davis et al. (2006) investigated heat lamp energy distribution using infrared thermography for various heat lamp outputs and heights above the floor. They found that heat lamps, even at the same rated output, produce varying temperature profiles at the floor and that the shape of the lens greatly affects this heat distribution. They found that by using a heat lamp output power controller they could effectively adjust the floor heating pattern while at the same time achieving overall energy reduction and that by varying the energy output at a given lamp height, the need to adjust lamp height diminished. Houszka et al. (2001) showed the importance of creep area design on overall micro-climate control without the need for supplemental creep area heating. Wheeler et al. (2008) studied the space occupied by piglets in the creep area of a farrowing crate to variations in heat lamp output affecting floor temperature. They found that average floor temperatures of 34°C, 27°C, and 25°C were found to be preferred for piglet comfort at weeks 1, 2, and 3, respectively. Hoff (2003) showed preliminary evidence that a shielded temperature sensor could be used in the heating zone of a flame-based IR heater to adequately sense the average AOZ temperature.

Surface Characteristics as Influenced by Radiant Heat

Knowing the wavelength of maximum IR emission is important because it defines the emission surface properties at the IR heater source, and the absorptive properties of any object receiving this energy. For most flame-based IR heaters, the emitting surface is typically perforated oxidized iron that has a reported emissivity at a surface temperature of 1472 K (λ_{max}=1.97 μm) of about 0.89 (Omega Engineering, Inc., 2008). Hall (1962) proposed an IR emitting surface emissivity of 0.90 for a lack of better data. For receivers, the absorptivity at the incident wavelength (i.e. from the IR source) is important and this surface property is also dependent upon the source wavelength of maximum emission. Kuppenheim et al. (1956) studied in detail the reflective (ρ) properties of Chester White pigs for incident wavelengths between 0.20 and 2.6 μm. Incident IR energy in the NIR has a maximum emission at a wavelength of about 1.1 μm. If one assumes that the transmitted IR energy is zero, then the absorptivity (α) can be determined as (1-ρ) and based on Kuppenheim et al.'s (1956) research, the reflectivity at 1.1 μm was measured at 0.30 implying that the absorptivity at this wavelength is approximately 0.70. Once absorbed, a pig will reemit IR energy to the surroundings at a reduced temperature representative of the pig's skin temperature. If one assumes a skin temperature of 308 K (35°C), the wavelength of maximum reemission is about 9.5 μm, or in the LWIR range. Although beyond the 2.6-μm wavelength studied by Kuppenheim et al. (1956), the reflectivity from their study was shown to reduce dramatically after λ=1.7 μm and remained constant at approximately 0.09 implying that the absorptivity (or emissivity at this temperature) is about 0.91.

Summary

The literature cited on the topic of IR heating indicates that models or experiments intended to simulate IR heating in the AOZ need to incorporate, in the absence of animals themselves, absorption surfaces in the AOZ of about 0.70 at an incident wavelength of about 1.1 μm and reemission surfaces in the AOZ of about 0.91 in accordance with the wavelength of maximum emission of NIR sources used for micro-climate control. In addition, the micro-climate can be effectively changed by adjusting the energy input to the AOZ with realized energy savings but that the need exists to be able to sense the AOZ micro-climate to provide feedback control.

Objectives

The specific objectives of this research project were to:

- develop a simplified theoretical analysis of the IR heating zone and expected response of a sensor placed in the IR heating zone,
- develop a prototype IR sensor using guidelines established with objective one,
- using a prototype IR sensor, determine the adequacy of describing the average temperature for animals in the IR heating zone, and,
- quantify the dynamic response of the prototype IR sensor.

Theoretical Expectations

A simplified theoretical analysis of the IR heating process was conducted to gain insights into the development of a sensor capable of representing the AOZ as affected by IR heating. The main goal was to determine if a single sensor location could be used to sense the AOZ heating environment and whether this single location would respond accordingly with variations in IR heater output.

IR Heat Distribution to the AOZ

In general, IR energy will be emitted from a flame-based heater with a theoretical maximum output described by the Stefan-Boltzman relationship as (see nomenclature for variable definitions):

$$Q_h = A_h \sigma T_h^4 \quad (1)$$

For a perfect stoichiometric combustion of LP in air (T_h=2253 K; Barnard and Bradley, 1985) and perfectly transferred to an emitting surface with an emissivity (ε) of 1, the absolute maximum radiant flux (W/m^2) that can be delivered with an LP-based IR heater is:

$$\frac{Q_h}{A_h} = \sigma T_h^4 = (5.67\times10^{-8})(2253)^4 = 1{,}460{,}925\frac{W}{m^2} \quad (2)$$

Equations 1 and 2 assume that the heater is a perfect emitter (ε=1) and that the combustion process results in a perfect conversion of fuel to a representative surface temperature for emission, neither of which exists in practice. A revised form of equation 1 to account for these inefficiencies is represented as:

$$Q_h = \frac{A_h \varepsilon_h \sigma T_h^4}{\eta_h} \quad (3)$$

where now the imperfect emitter characteristics (ε_h<1) and the combustion inefficiency (η_h<1) has been accounted for. Hall (1962) proposed an emission efficiency for flame-based IR heaters of ε_h=0.90 which agrees closely with the ε=0.89 value for oxidized metal summarized in Omega Engineering, Inc., (2008). The flame-based inefficiency is much more difficult to determine but a tentative value of η_h=0.60 was assigned for the analysis that follows. Based on the assigned parameters, a flame-based IR heater would be expected to have an emission surface temperature (K) of:

$$T_h = \left\{ \frac{Q_h \eta_h}{A_h \varepsilon_h \sigma} \right\}^{0.25} \tag{4}$$

Knowing the consumed fuel of the heater would allow for a prediction of the IR heating temperature. For example, if a 10-cm diameter IR heater consumes 1,000 W (3,412 Btu/h) of fuel, the predicted IR heating surface would reach a temperature of:

$$T_h = \left\{ \frac{Q_h \eta_h}{A_h \varepsilon_h \sigma} \right\}^{0.25} = \left\{ \frac{1{,}000(0.60)}{\left(\frac{\pi(0.10^2)}{4} \right)(0.90)(5.67 \times 10^{-8})} \right\}^{0.25} = 1{,}106K = 833C \tag{5}$$

Ibrahim and Briselden (2002) reported that most flame-based IR heaters operate at emission surface temperatures between 588 and 923 K (315 and 650°C) although improvements to the emission surface design can improve this to 1473 K (1200°C). Shilton et al (2002) reported an emitter temperature of 767 K (494°C)for a gas-fired catalytic plaque IR heater.

An IR heater will administer energy to the AOZ as a function of the spatial orientation between the IR heater and the position of animals in the AOZ. Theoretically, this relationship can be accounted for by the shape factor (Modest, 1993; Holman, 2002) between the IR heater and the location of animals in the AOZ. Assuming a parallel (to the floor) circular IR heater at some elevation *Y* above the floor, the energy that impinges upon a ring of radius *R* from the center-line of the heating zone can be represented as (Modest, 1993):

$$Q_{floor,r} = Q_h F_{h-floor,r} \tag{6}$$

The shape factor $F_{\text{h-floor,r}}$ can be determined using the relationship between an assumed circular source and a coaxially-located ring located at some elevation *Y* and radial distance *R* from the circular source. The relationship modeled is shown in figure 1 with the shape factor $F_{\text{h-floor,r}}$ determined using the following set of relationships (Modest, 1993):

$$R_1 = \frac{R_h}{Y}$$

$$R_2 = \frac{R_o}{Y}$$

$$R_3 = \frac{R_i}{Y}$$

$$X_1 = 1 + \frac{1 + {R_2}^2}{{R_1}^2}$$

$$X_2 = 1 + \frac{1 + {R_3}^2}{{R_1}^2}$$

$$F_{h-floor,r} = \frac{1}{2}\left\{ X_1 - \sqrt{{X_1}^2 - 4\left(\frac{R_2}{R_1}\right)^2} \right\} - \frac{1}{2}\left\{ X_2 - \sqrt{{X_2}^2 - 4\left(\frac{R_3}{R_1}\right)^2} \right\} \tag{7}$$

The actual flux of energy impinging upon this ring can be described as:

$$q_{floor,r} = \frac{Q_{floor,r}}{A_{floor,r}} = \frac{Q_h F_{h-floor,r}}{A_{floor,r}} \tag{8}$$

A portion of the IR energy that impinges upon this ring will be absorbed as:

$$q_{absorbed,floor,r} = \alpha_{floor} \frac{Q_h F_{h-floor,r}}{A_{floor,r}} \tag{9}$$

The absorbed radiant energy at the floor at some radius *R* will be redistributed to the surroundings by reemission of radiant energy by convection or by conduction through the receiver located at this ring. Assuming conduction through the receiver to be small relative to the reemission of radiant energy and the heat transferred *via* convection, the surface temperature of the receiver ($T_{\text{floor,r}}$) can be determined by solving the following mixed-mode energy balance at the receiver:

$$q_{absorbed,floor,r} = h_{floor}(T_{floor,r} - T_\infty) + \varepsilon_{floor,r}\sigma({T^4}_{floor,r} - {T^4}_\infty) \tag{10}$$

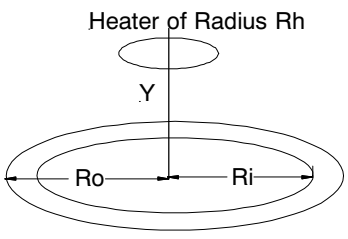

Figure 1. Relationship between a circular IR heater located Y above the floor for various radii from the IR heater center-line.

Equation 10 assumes that the room is well insulated allowing for the surrounding surface temperatures driving radiative reemission to be reasonably equal to the surrounding air temperature that drives the convection process; a reasonable assumption for the simplified analysis given.

A hypothetical case was chosen to determine the expected heating pattern and to test various sensor locations within the IR heating zone. The hypothetical case chosen was a 25 cm diameter (R_h=12.5 cm) heater consuming 3,000 W (Q_h) and located 75 cm above the floor (Y). To analyze this hypothetical case, 5-cm (2-in.) rings (R_o-R_i) were used to discretize and analyze the IR heating zone, the results of which are given in table 1. The analysis given in table 1 was carried out to a radius of 127 cm (50 in.). The assumed radiative surface properties used for the results in table 1 were α_{floor} =0.70 and ε_{floor} =0.91, consistent with a pig's skin surface properties, mimicking animals present in the AOZ. The convective heat transfer coefficient was assumed to be h_{floor}=5 W/m^2-K, a reasonable assumption for analysis purposes.

Table 1 shows important information relative to the analysis given previously. The 5-cm (2-in.) ring under consideration is given in each row of table 1. The ring area, shape factor (eq. 7), radiant energy incident on each ring (eq.6), the flux of radiant energy on each ring (eq. 8), and the resulting average ring temperature (solved eq. 10) is given for this hypothetical case. In addition, an averaged heating zone temperature is given referred to here as the Area Weighted Average Temperature (AWAT) defined as:

$$AWAT = \frac{\sum_{i=1}^{25} T_i A_i}{A_t} \quad (11)$$

Table 1 also indicates the sum of the shape factor from the IR heater to the floor for the maximum radius of 127 cm (50 in.) used in the analysis. This summation $\Sigma F_{h\text{-}floor,r}$=0.734 implies that 73.4% of the emitted IR energy from the modeled IR heater has been accounted for in this 127-cm radius ring around the heater, at the floor, implying further that a larger outer diameter is required to capture all of the incident IR energy from the heater.

IR Sensor Response in the IR Heat Pattern

The set-up and analysis given above was used to assess the feasibility of placing a sensor, within the IR heating zone, to sense the AWAT in the AOZ for variable IR heating rates

Table 1. Theoretical expectation of the floor temperature as a function of distance from heater center-line.[a]

Ring Outer Radius, cm (in.)	Ring Inner Radius, cm (in.)	Ring Area, cm^2 (in.^{2})	$F_{h\text{-}floor,r}$[b]	Energy at Ring, W[c]	Flux at Ring, W/m^2[d]	Ring Temperature, °C[e]
127 (50)	122 (48)	3974 (616)	0.016	29.7	52.4	25.0
122 (48)	117 (46)	3813 (591)	0.018	32.2	59.1	25.7
117 (46)	112 (44)	3645 (565)	0.019	34.8	66.7	26.4
112 (44)	107 (42)	3484 (540)	0.021	37.6	75.6	27.2
107 (42)	102 (40)	3323 (515)	0.022	40.7	85.7	28.2
102 (40)	97 (38)	3161 (490)	0.024	44.0	97.4	29.3
97 (38)	92 (36)	3000 (465)	0.026	47.5	110.9	30.5
91 (36)	86 (34)	2839 (440)	0.028	51.2	126.4	32.0
86 (34)	81 (32)	2677 (415)	0.030	55.1	144.2	33.6
81 (32)	76 (30)	2516 (390)	0.032	59.1	164.5	35.5
76 (30)	71 (28)	2348 (364)	0.035	63.1	187.8	37.5
71 (28)	67 (26)	2187 (339)	0.037	67.0	214.2	39.8
66 (26)	61 (24)	2026 (314)	0.039	70.7	244.1	42.5
61 (24)	56 (22)	1865 (289)	0.041	73.9	277.4	45.3
56 (22)	51 (20)	1703 (264)	0.042	76.4	314.3	48.5
51 (20)	47 (18)	1542 (239)	0.043	78.0	354.5	51.8
46 (18)	41 (16)	1381 (214)	0.043	78.3	397.5	55.4
41 (16)	36 (14)	1213 (188)	0.042	76.9	442.5	59.0
36 (14)	31 (12)	1052 (163)	0.040	73.5	488.3	62.6
30 (12)	25 (10)	890 (138)	0.037	68.0	533.4	66.1
25 (10)	20 (8)	729 (113)	0.033	60.0	575.8	69.3
20 (8)	15 (6)	568 (88)	0.027	49.7	613.3	72.1
15 (6)	10 (4)	406 (63)	0.020	37.3	643.9	74.4
10 (4)	5 (2)	245 (38)	0.013	23.1	665.5	75.9
5 (2)	0	84 (13)	0.004	7.8	676.7	76.8
		$\Sigma F_{h\text{-}floor,r}$ =	0.734		AWAT:	36.8

[a] IR heater assumed to be 60% efficient and rated at a consumption of 3,000 W. IR heater located 75 cm above the floor. Floor assumed to absorb IR energy (1.2-μm wavelength) at α = 0.70 and reemit at an emissivity ε = 0.91 (9.5-μm wavelength) consistent with results from Kuppenheim et al. (1956).
[b] Shape factor from heater to ring at radius r (eq. 7).
[c] Infrared energy incident upon ring at radius r (eq. 6).
[d] Infrared energy per unit surface area at radius r (eq. 8).
[e] Estimated temperature of ring located at r (solved eq. 10).

without changing the position of the sensor. If this scenario is theoretically possible, then the development of a practical IR sensor should be possible in practice. To test this scenario a fictitious sensor was placed in the IR heating zone as shown in figure 2.

This sensor, of length L, will occupy a ring within the IR heating zone similar to the 5-cm rings discretized at the floor to represent the AOZ. The shape factor that describes the ring that occupies the sensor of length L can be determined as follows:

$$R_1 = \frac{R_h}{y}$$

$$R_2 = \frac{S_o}{y}$$

$$R_3 = \frac{S_i}{y}$$

$$X_1 = 1 + \frac{1 + {R_2}^2}{{R_1}^2}$$

$$X_2 = 1 + \frac{1 + {R_3}^2}{{R_1}^2}$$

$$F_{h-sensor,r} = \frac{1}{2}\left\{X_1 - \sqrt{{X_1}^2 - 4\left(\frac{R_2}{R_1}\right)^2}\right\} - \frac{1}{2}\left\{X_2 - \sqrt{{X_2}^2 - 4\left(\frac{R_3}{R_1}\right)^2}\right\} \quad (12)$$

This shape factor describes the energy incident upon the entire ring of width L located *y* below the IR heater. Dividing this incident energy by the ring area represents the flux of energy experienced by the sensor. This relationship can be described as:

$$q_{absorbed,sensor,r} = \alpha_{sensor} \frac{Q_h F_{h-sensor,r}}{A_{ring,r}} \quad (13)$$

As with animals located in the AOZ, the sensor will reach some steady-state (SS) temperature based on the net exchange between the IR energy absorbed and the radiant and convective energy released as:

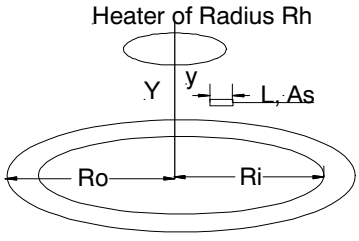

Figure 2. Relationship between a circular IR heater located Y above the floor for various radii from the IR heater center-line and a sensor placed at some intermediate distance y below the IR heater.

$$q_{absorbed,sensor} = h_{sensor}(T_{sensor} - T_\infty) + \varepsilon_{sensor}\sigma\left({T^4}_{sensor} - {T^4}_\infty\right) \quad (14)$$

A successful IR sensor will be one that reaches a SS temperature representative of the AWAT experienced in the AOZ, and, changes SS temperature response analogous to the AOZ for changes in IR heater output without repositioning the sensor. To test the theoretical expectations of a proposed IR sensor, the case given in figure 2 was analyzed for the heater results presented in table 1.

A series of sensor placements were tested based on the case given in figure 2 for the heating results given in table 1. The fictitious sensor tested was 2.5 cm (1 in.) long and had an assumed absorptivity of 0.30. Table 2 summarizes the results from this exercise.

Table 2 shows the results for the sensor placed at *y*=25, 38, and 51 cm below the IR heater (located *Y*=75 cm above the floor). The 2.5-cm long sensor was then analyzed for placements between 5 and 40 cm radially outward from the heater center-line. A careful review of the anticipated sensor temperatures indicates that for all of the tested IR sensor locations, the sensor would record a temperature substantially higher than the AWAT for the heater analyzed in table 1. This exercise indicated that a sensor, with an assumed absorptivity of 0.30, would need to be lowered very near the floor and outward from the heater to reach a location where the SS temperature would represent the AWAT of the AOZ. Both of these options are unacceptable in practice with animals present.

Two options exist to remedy this situation. The first is to select a sensor that has an absorptivity substantially lower than the assumed 0.30 used for the results shown in table 2. However, an absorptivity less than 0.30 would require a sensor surface that remained in a pristine reflective state for long periods of time, a requirement that is unrealistic in animal housing applications. An alternative approach is to reduce the IR energy experienced by the sensor at any given location within the IR heating zone while still maintaining the sensor at an ample elevation above the AOZ. One solution is to shield the IR sensor with a material that physically reduces the exposure from the IR heater, with an air space separating the shield from the IR sensor. In theory, a shield will reduce the radiative flux at a receiver by $(n+1)^{-1}$ where n is the number of shields (Holman, 2002). A single shield (n=1) was adopted as a possible remedy for an IR sensor to be placed within the IR heating zone. The hypothetical results of a single shield surrounding the IR sensor are given in table 3. The flux arriving at the shielded sensor has been assumed to be 50% of the unshielded case (table 2) in accordance with theory (Holman, 2002). As shown in table 3, shielding the sensor (with one shield) has provided for a SS temperature close to the AWAT of 41.1°C for the heating conditions given in table 1.

The results shown in table 3 indicate that a shielded IR sensor should be able to successfully represent the AWAT and be placed at a satisfactory distance above the floor to remain free from AOZ interference. The key remaining requirement was to determine if the shielded IR sensor, located at a fixed location relative to the IR heater, would respond adequately to changes in the AWAT as a result of IR heater output changes. Table 4 shows the results of this exercise. A placement was located for the results given in table 3 where

Table 2. Theoretical expectation of an IR sensor located within the IR heating zone to represent the AWAT for the conditions summarized in table 1.[a]

Sensor Distance below Heater, cm (in.)	Sensor Outer Radius, cm (in.)	Sensor Inner Radius, cm (in.)	$F_{h\text{-sensor ring}}$	Energy at Sensor Ring, W	Flux at Sensor, W	Sensor Temperature, °C
25 (10)	5 (2)	2.5 (1)	0.023	42.0	2,065.0	233.6
	10 (4)	7.5 (3)	0.048	86.0	1,820.0	215.4
	15 (6)	12.5 (5)	0.060	109.0	1,463.0	186.2
	20 (8)	17.5 (7)	0.061	110.0	1,089.0	151.8
	25 (10)	22.5 (9)	0.055	99.0	769.0	118.7
	30 (12)	27.5 (11)	0.046	82.0	529.0	91.0
	35 (14)	32.5 (13)	0.037	66.0	362.0	70.1
	40 (16)	37.5 (15)	0.029	52.0	250.0	55.3
38 (15)	5 (2)	2.5 (1)	0.012	21.0	1,047.0	147.7
	10 (4)	7.5 (3)	0.026	46.0	975.0	140.5
	15 (6)	12.5 (5)	0.036	64.0	863.0	128.8
	20 (8)	17.5 (7)	0.041	74.0	729.0	114.2
	25 (10)	22.5 (9)	0.042	76.0	594.0	98.8
	30 (12)	27.5 (11)	0.041	73.0	472.0	84.0
	35 (14)	32.5 (13)	0.037	67.0	368.0	70.9
	40 (16)	37.5 (15)	0.033	60.0	285.0	60.0
51 (20)	5 (2)	2.5 (1)	0.007	13.0	620.0	101.8
	10 (4)	7.5 (3)	0.016	28.0	594.0	98.7
	15 (6)	12.5 (5)	0.023	41.0	550.0	93.5
	20 (8)	17.5 (7)	0.028	50.0	494.0	86.7
	25 (10)	22.5 (9)	0.031	56.0	433.0	79.1
	30 (12)	27.5 (11)	0.032	58.0	371.0	71.3
	35 (14)	32.5 (13)	0.032	57.0	313.0	63.7
	40 (16)	37.5 (15)	0.030	55.0	261.0	56.8

[a] Fictitious sensor tested had a length of 2.5 cm (1 in.) and an assumed absorptivity to 1.2-μm wavelength of 0.30.

the shielded IR sensor described the AWAT at 100% IR heater output. The placement found was a sensor vertical location below the IR heater of 23 cm (9 in.) and a radial distance of 41 cm (16 in.). This was the fixed location chosen for the results given in table 4. The results given in table 4 indicate that a shielded IR sensor, located within the IR heating zone, should be able to represent the AWAT for the animals in the AOZ held at a fixed location and subjected to a variable output IR heating system. The theoretical assessment gave confidence in the development of such a sensor.

Materials and Methods

An experimental set-up was devised to test the practical use of a shielded IR sensor in accordance with theoretical expectations. The basic experimental set-up is shown in figure 3. A 15-cm (6-in.) thick concrete floor along with 91-cm (36-in.) high concrete sub-floor panels spaced at 2.44 m (8 ft) were used to simulate a basic infrared heating zone. To sense animal conditions at the floor, 5.1- × 7.6- × 30.5-cm (2- × 3- × 12-in.) rain gutter down-spout sections were used, installed with two T-type thermocouples (TC) at the underside of the top section. The cavity of each simulated pig (SimPig) was filled with fiberglass batt insulation (fig. 4). The outer surface of each SimPig was painted with a flat-gray enamel paint to provide absorptive and emissive characteristics reasonably representative of a pig's surface ($\alpha = \varepsilon$ ~0.90-0.95; Raytek, Inc., 2008). Ten total SimPigs were constructed to sense the IR heating zone. In addition to the SimPig temperatures, an ambient air temperature called "pen air" was measured at 122 cm (48 in.) above the floor and 30 cm (12 in.) horizontally removed from the nearest point of the IR heater. Temperature data was recorded at 5-min intervals with a commercially available data logger (Model CR-10, Model AM-416; Campbell Scientific, Inc., Logan, Utah).

Infrared heaters available for animal housing applications were chosen to test the developed IR sensor (Models M-3, M-5, M-8; Gasolec, Inc., Fairseat Kent, United Kingdom). The control system used for testing the IR sensor was the Ventium® Control Center (CC; v2.04) complete with an output module (OM) for relay control, an input module (IM) for sensor acquisition, and a base module (BM) for communication protocol. This control system was used to

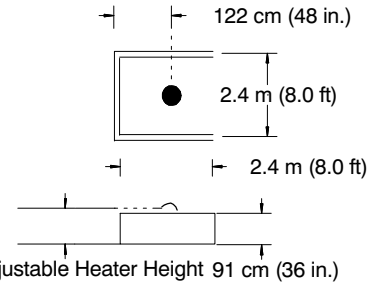

Figure 3. Simulated pen area and IR heater set-up. Flooring was 15-cm (6-in.) thick concrete and sidewall and end panels were constructed from 1.3-cm (0.5-in.) concrete panels.

Table 3. Theoretical expectation of a shielded IR sensor located within the IR heating zone to represent the AWAT for the conditions summarized in table 1. [a][b]

Sensor Distance below Heater, cm (in.)	Sensor Outer Radius, cm (in.)	Sensor Inner Radius, cm (in.)	$F_{h\text{-sensor ring}}$	Energy at Sensor Ring, W	Flux at Shielded Sensor, W	Shielded Sensor Temperature, °C
25 (10)	5 (2)	2.5 (1)	0.023	42.0	1,032.5	146.2
	10 (4)	7.5 (3)	0.048	86.0	910.0	133.8
	15 (6)	12.5 (5)	0.060	109.0	731.5	114.5
	20 (8)	17.5 (7)	0.061	110.0	544.5	92.8
	25 (10)	22.5 (9)	0.055	99.0	384.5	73.0
	30 (12)	27.5 (11)	0.046	82.0	264.5	57.3
	35 (14)	32.5 (13)	0.037	66.0	181.0	**45.9**
	40 (16)	37.5 (15)	0.029	52.0	125.0	**38.0**
38 (15)	5 (2)	2.5 (1)	0.012	21.0	523.5	90.3
	10 (4)	7.5 (3)	0.026	46.0	487.5	86.0
	15 (6)	12.5 (5)	0.036	64.0	431.5	79.0
	20 (8)	17.5 (7)	0.041	74.0	364.5	70.5
	25 (10)	22.5 (9)	0.042	76.0	297.0	61.6
	30 (12)	27.5 (11)	0.041	73.0	236.0	53.4
	35 (14)	32.5 (13)	0.037	67.0	184.0	**46.3**
	40 (16)	37.5 (15)	0.033	60.0	142.5	**40.5**
51 (20)	5 (2)	2.5 (1)	0.007	13.0	310.0	63.3
	10 (4)	7.5 (3)	0.016	28.0	297.0	61.6
	15 (6)	12.5 (5)	0.023	41.0	275.0	58.7
	20 (8)	17.5 (7)	0.028	50.0	247.0	54.9
	25 (10)	22.5 (9)	0.031	56.0	216.5	50.8
	30 (12)	27.5 (11)	0.032	58.0	185.5	46.5
	35 (14)	32.5 (13)	0.032	57.0	156.5	**42.5**
	40 (16)	37.5 (15)	0.030	55.0	130.5	**38.8**

[a] Fictitious sensor tested had a length of 2.5 cm (1 in.) and an assumed absorptivity to 1.2-μm wavelength of 0.30.
[b] Bolded results indicate conditions reasonably representing the AWAT of 41.1°C from table 1.

Table 4. Theoretical expectation of an IR sensor located within the IR heating zone to represent the AWAT for the conditions summarized in table 1 with a variable output IR heater. [a]

Sensor Distance Below Heater, cm (in.)	Sensor Outer Radius, cm (in.)	Sensor Inner Radius, cm (in.)	$F_{h\text{-sensor ring}}$	IR Heater Consumption, W	AWAT, °C	Shielded IR Sensor Temperature, °C
23 (9)	41 (16)	38 (15)	0.027	3,000	36.8	36.8
				2,500	34.1	34.0
				2,000	31.4	31.3
				1,500	28.7	28.4
				1,000	25.8	25.6
				500	22.9	22.7
				250	21.4	21.3
				0	20.0	20.0

[a] Fictitious sensor tested had a length of 2.5 cm (1 in.) and an assumed absorptivity to 1.2-μm wavelength of 0.30.

control a custom-made liquid propane (LP) gas modulation system (Ray Dot, Inc., Cokato, Minn.). The gas modulation set-up is shown in figure 5. The IR heater control and gas modulation system provided three basic heating levels consisting of: pilot only (P), pilot + low (PL), and pilot + low + high (PLH). The LP modulated heaters were set to deliver operating gas pressures of 1.0, 2.5, and 5.0 psi for the P, PL, and PLH control settings, respectively.

The 10 SimPigs were arranged in the IR heating zone as shown in figure 6. One of the SimPigs was placed well outside the heating zone and was used as a reference (SimPig 1, fig. 6). The heating area represented by the SimPigs was

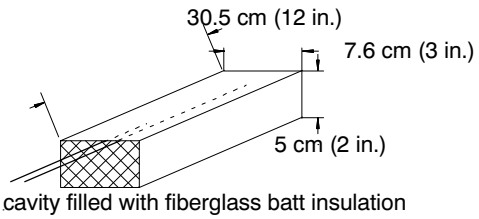

Figure 4. Set-up for the simulated pigs. Two thermocouples (T-type) placed at inside top surface 5 cm (2 in.) from each end.

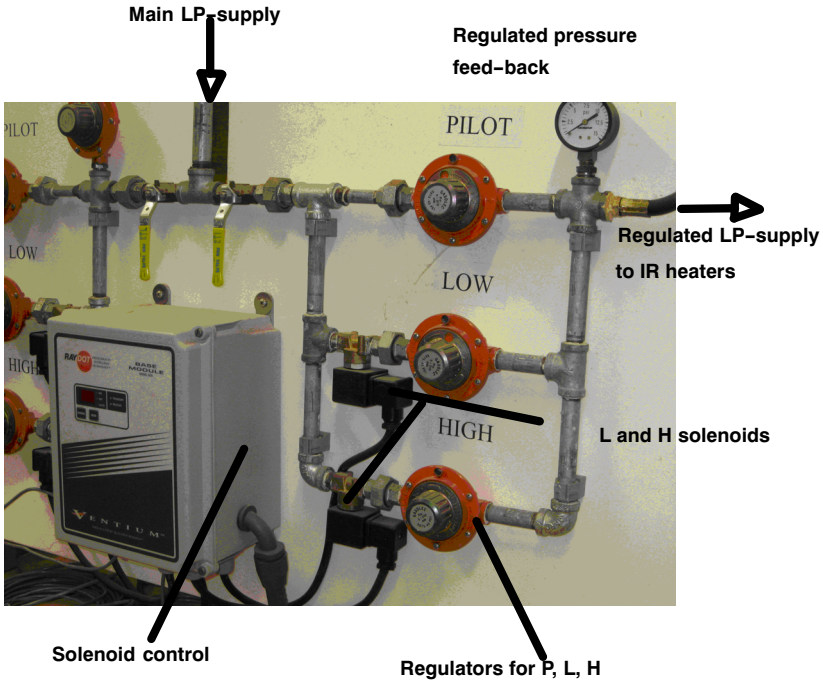

Figure 5. Gas modulation set-up. Low (L) and High (H) regulated settings controlled via solenoids with Pilot (P) manually on. Regulators used to provide 1.0-, 2.5-, and 5.0-psi LP-gas pressures for the P, L, and H settings, respectively.

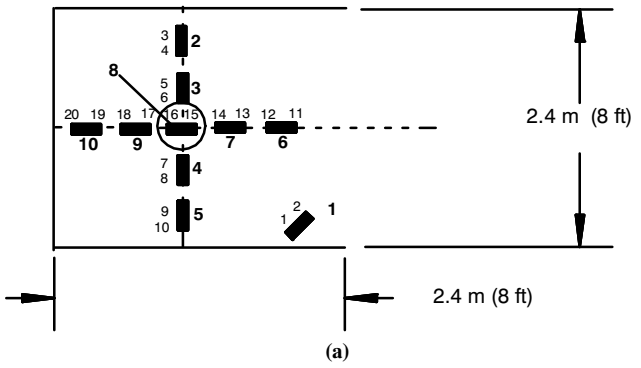

(a)

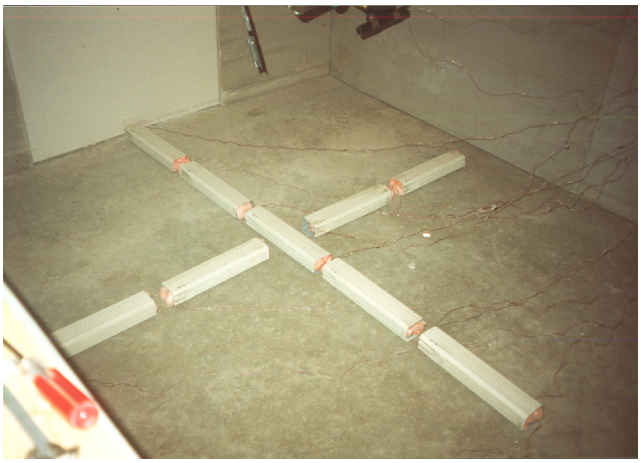

(b)

Figure 6. Simulated pigs used for assessing thermal conditions experienced in the IR heating zone. (a) Indicates each of the 10 SimPigs with the 20 TC sensor designations and (b) the layout of the SimPigs as tested (SimPig 1 not visible in photograph).

discretized by paired thermocouple (TC) locations (fig. 6) to yield a representative AWAT analogous to the AWAT described and used in the theoretical analysis. The TC designations and radii associated with each TC pair are given in table 5.

The AWAT was calculated as:

$$AWAT = \frac{\sum_{i=1}^{9}\left\{\frac{1}{2}\left(TC_j + TC_{j+1}\right)\left(A_i\right)\right\}}{A_t} \quad (15)$$

IR Prototype Sensor

The IR sensor developed and tested is shown in figure 7 and represents a simplified version of a shielded sensor (n=1) proven to work theoretically for this application. The IR sensor consisted of an RTD temperature sensor 5 mm in diameter and 25 mm in length placed at the center of a 1.3-cm inside diameter electrical conduit galvanized metal pipe

Table 5. Thermocouple (TC) placement and radii associated with each placement.

Region ID	TC Sensors[a]	Radius, cm (in.)	Net Region Area, cm^2 (in.^{2})
1	15, 16	10 (4)	325 (50)
2	6, 7	18 (7)	671 (104)
3	14, 17	30 (12)	2,252 (349)
4	5, 8	43 (17)	(3,606 (559)
5	13, 18	53 (21)	5,329 (826)
6	4, 9	64 (25)	7,335 (1,137)
7	12, 19	71 (28)	8,555 (1,326)
8	3, 10	86 (34)	14,877 (2,306)
9	11, 20	97 (38)	14,394 (2,231)

[a] See figure 6A.

Figure 7. IR sensor prototype developed and tested.

(α=ε ~0.23 new, =0.88 old at 300 K; The Engineering Toolbox, 2008). The RTD was fixed at the center with a small copper wire to provide an air space between the RTD and the shield; a critical requirement for IR shielding. The RTD behaved like a shielded sensor with exposure to room air from the back-side of the sensor.

To accommodate IR sensor placement testing, a support bracket was designed that simultaneously supported the IR sensor and allowed for easy placement into and out-of the IR heating zone (fig. 8). The bracket was fitted to the existing IR heater bracket and allowed for a single pivot-point that placed the IR sensor into and away from the IR heating zone. The sensor placement resulted in an angled IR sensor within the IR heating zone which was different from the theoretical case analyzed where a parallel sensor placement was modeled. This difference however is not important in practice. The importance is in having the ability to physically move the IR sensor into and out of the IR heating zone to locate one representative location for the IR sensor in relation to the AWAT. Rotating the pivot arm of the IR sensor bracket allowed for a variety of positions to be tested. The semi-circular gage shown on the IR sensor bracket allowed for reproducibility in pivot location as each IR heater was tested at various heights above the floor.

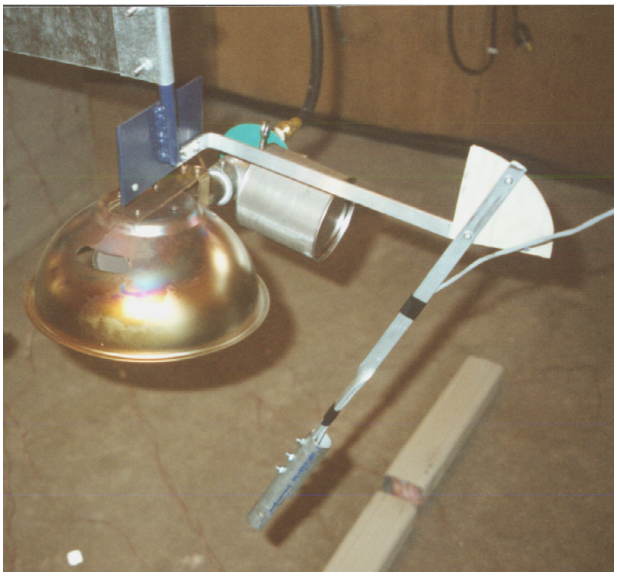

Figure 8. IR sensor bracket developed and used for testing IR sensor placement within the heating zone. The M-3 (Gasolec, Inc., Fairseat Kent, UK) heater shown.

The testing procedures involved a significant amount of trial and error to prove that the IR sensor captured the AWAT and that a single representative IR sensor placement location could be found as was shown in theory. A series of runs were conducted with the M-3, M-5, and M-8 IR heaters, with each placed at various heights above the floor. The goal was to find an IR sensor placement position for each combination of IR heater capacity and heater height that sensed the AWAT and was insensitive to IR heater output changes. In practice, each IR heater will have an ideal placement height above the AOZ mainly as a function of IR heater output and pen layout. The tests conducted with this research did not attempt to find an "ideal" IR heater height. Instead, the goal was to prove whether or not a shielded IR sensor could be positioned for a given IR heater height that sensed the AWAT accurately and that was insensitive to IR heater output at a fixed IR heater height.

The overall procedure was to select an IR heater (M-3, M-5, or M-8), select a representative IR heater height (*Y*), and then using the IR sensor bracket system find a location that best represents the AWAT for the IR heater at a heater output set to PLH. Once found, the IR sensor, remaining fixed, was then tested against the P and PL gas modulation settings for adequacy as a feedback IR sensor as dictated by IR response in relation to the measured AWAT (eq. 15).

Results and Discussion

IR Heating Pattern

The 10 SimPigs gave feedback on the energy distribution in the IR heating zone similar to the heating "rings" used in the theoretical analysis (see fig. 1). Figure 9 is an example of the SimPig response to various LP gas modulating settings as modulation was changed from P, then to PL, then to PLH, and finally back to P. Selected SimPigs and SimPig temperatures are identified relative to the layout shown in figure 6A. Clearly, the SimPigs gave excellent feedback response to changes in LP gas modulation.

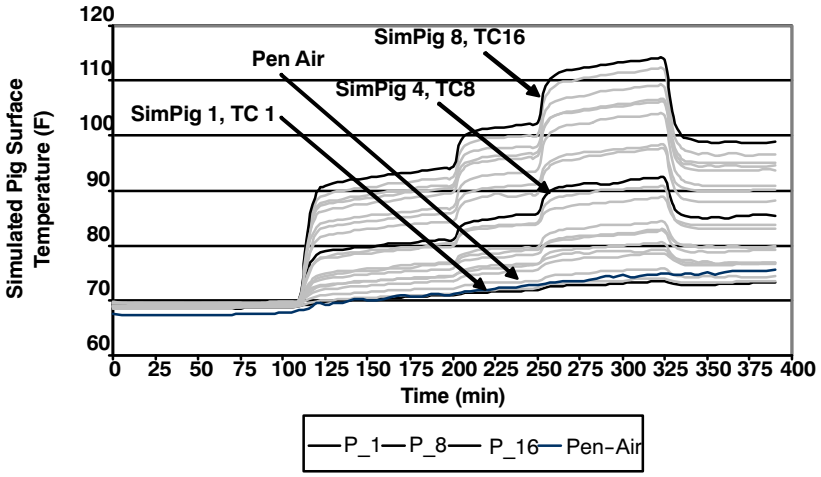

Figure 9. SimPig response to IR heater settings for P, PL, and PLH settings.

The AWAT as a Representative IR Heating Zone Temperature

The heating patterns of the SimPigs as shown in figure 9 were summarized with the AWAT (eq. 15) in a similar manner to the theoretical assessment described earlier. The AWAT response for the experimental set-up given in figure 9 is shown in figure 10.

Several tests were conducted to test the M-3, M-5, and M-8 heaters using the pivoting variations available with the IR sensor bracket developed. Several trial and error tests were conducted to locate a single IR sensor location that behaved in a similar manner to the theoretical expectations described earlier. For all IR heaters tested, and all heater heights tested, a representative IR sensor position was found that described the AWAT for variations in IR heater output; a result analogous to theoretical expectations. A sample result is given in figure 11 for the IR heater case given in figures 9 and 10. Figure 11 indicates that a fixed IR sensor placement was found that described the AWAT very well for variations in IR heater output, a result consistent with theoretical expectations. The results shown in figure 11 were for the M-5 heater at a heater height Y=102 cm (40 in.) above the floor. Similarly encouraging results were found for the M-3 and M-8 IR heaters.

IR Sensor Performance in Feedback Control

To be truly useful as a practical IR sensor, the IR sensor needs to perform adequately in a closed-loop negative feedback control algorithm to maintain a desired AWAT. Several control runs were made for each IR heater at selected IR heater heights using the fixed IR sensor location found from prior testing. The idea was to be able to select an IR heater, select an IR heater height, move the IR sensor to it's placement determined for this combination of IR heater height and type, select a desired AWAT set-point temperature, and allow the LP gas modulation system to perform this function with the developed IR sensor. Two of the results from this exercise are shown in figure 12.

Figures 12a,b demonstrate feedback control using the M-5 and M-8 IR heaters, respectively. Each graph includes the measured AWAT, the IR sensor response, the pen air temperature, and the average SimPig 1 temperature (average of TC1, TC2; see fig. 6A). For figure 12A, the M-5 heater at Y=102 cm (40 in.) was started at the 40-min mark and allowed to run manually at PLH. At the 75-min mark the gas was modulated to PL and remained manually in this mode until the 210-min mark. At the 210-min mark, the IR heater was allowed to enter automated feedback control using the IR sensor developed with a set-point temperature (SPT) of 79˚F. Between the 210- and 335-min marks, the M-5 heater

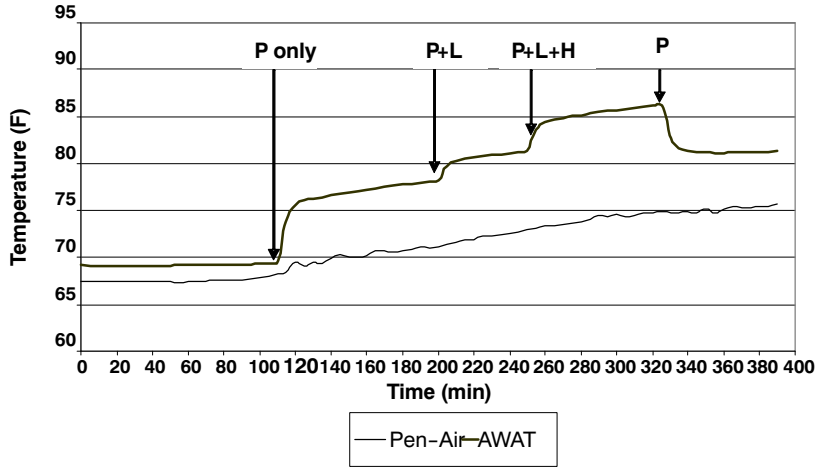

Figure 10. AWAT response of the SimPigs for the heater profile shown in figure 10.

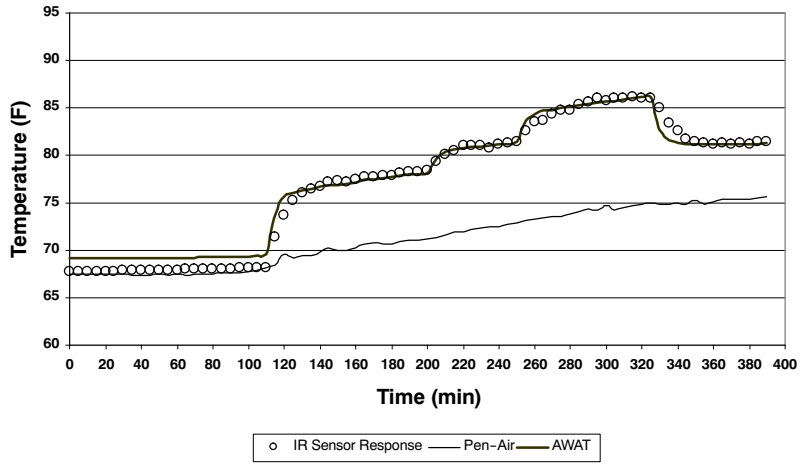

Figure 11. IR sensor representation of the AWAT for the heater profile shown in figure 10.

was in automated feedback control. The IR sensor provided adequate feedback of the AWAT maintaining the AWAT at 78.8±1.9°F (minutes 210-335). During the testing shown in figure 12a, the reference SimPig 1 was at roughly 64°F with the pen air oscillating between 63°F and 66°F, an artifact of the test room being controlled by it's own HVAC system.

Figure 12b shows an example feedback control run for the M-8 IR heater at *Y*=114 cm (45 in.). The M-8 heater shown in figure 12b was allowed to run manually at PL prior to the 50-min mark. At the 50-min mark, the gas supply to the M-8 heater was turned off and the cool-down process is evident. At the 65-min mark the M-8 heater was allowed to operate

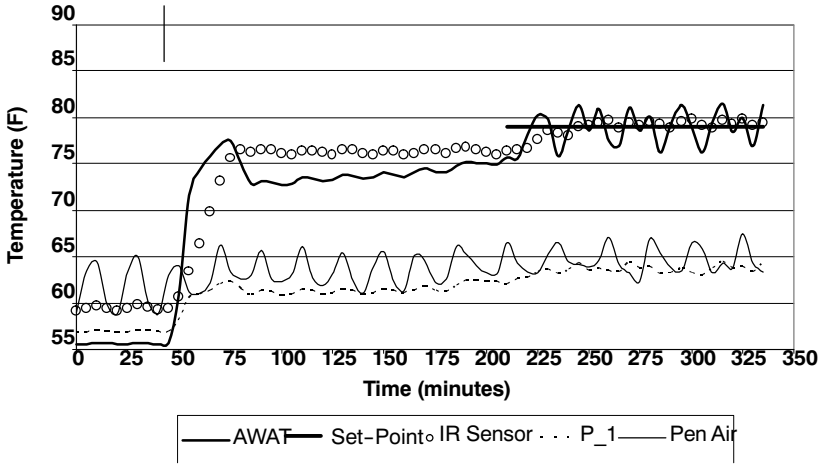

(a)

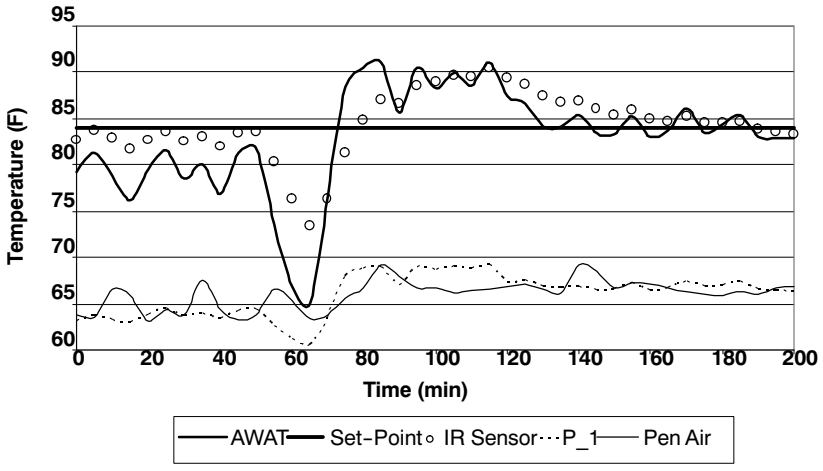

(b)

Figure 12. IR sensor in feedback control mode for (a) M-5 heater at *Y* = 102 cm (40 in.) with SPT = 79˚F initiated at the 210-min mark and (b) M-8 heater at *Y* = 114 cm (45 in.) with SPT = 84˚F initiated at the 110-min mark. See text for description of control runs shown.

manually at the PLH setting. Finally, at the 110-min mark, the M-8 heater was allowed to operate in feedback control mode using the developed IR sensor with a SPT=84°F and this proceeded until the 200-min mark. The IR sensor provided adequate feedback control of the AWAT maintaining the AWAT at 85.0±2.2°F (minutes 110-200).

IR Sensor Dynamic Characteristics

The feedback control runs shown in figure 12 indicated expected delays in the IR sensor response to changes in IR heater output. A common method for quantifying these delays is to specify the time constant, determined from a step-change in sensor input. Figure 13 shows the results of a step change in sensor input for both (a) heating and (b) cooling of the IR sensor. For both heating (fig. 13a) and cooling (fig. 13b), the IR sensor developed behaved as a first-ordered system as designated by the exponential response. The results from this testing indicated that the IR sensor had a heat-up time constant of 7.5 min and a cool-down time constant of 9.5 min.

Conclusions

The purpose of this research project was to develop a sensor that could be placed in the heating zone of an IR heater at a fixed location removed from animals and used to sense representative temperatures in the AOZ as changes to IR heater outputs were made. Ultimately, and if successful, the developed IR sensor could be used for feedback control of IR heaters. The results from this research resulted in the following conclusions:

- A theoretical assessment of IR heating indicated that a temperature sensor, exposed fully to the IR heating zone, could not be placed at a reasonable distance from the heater to represent the AWAT,
- A shielded IR sensor was shown theoretically to allow sensor placement at a reasonable location within the IR heating zone, removed from AOZ interference,
- Experimental results confirmed theoretical expectations in that a shielded IR sensor could be used, at a fixed location in the IR heating zone, to represent the AWAT for IR heaters with adjustable output settings,
- Experimental results confirmed the use of the developed shielded IR sensor to provide feedback control of the IR heating process, and,
- The experimental tests conducted indicated that the shielded IR sensor responds adequately to the actual AWAT in the AOZ and could be used successfully in field installations.

Acknowledgements

The author would like to thank Ray Dot, Inc. (Cokato, Minn.) for providing the Ventium® control system, the LP gas modulation system, and the Gasolec, Inc. (Fairseat Kent, UK) IR heaters used to conduct this research project. Their support is very much appreciated.

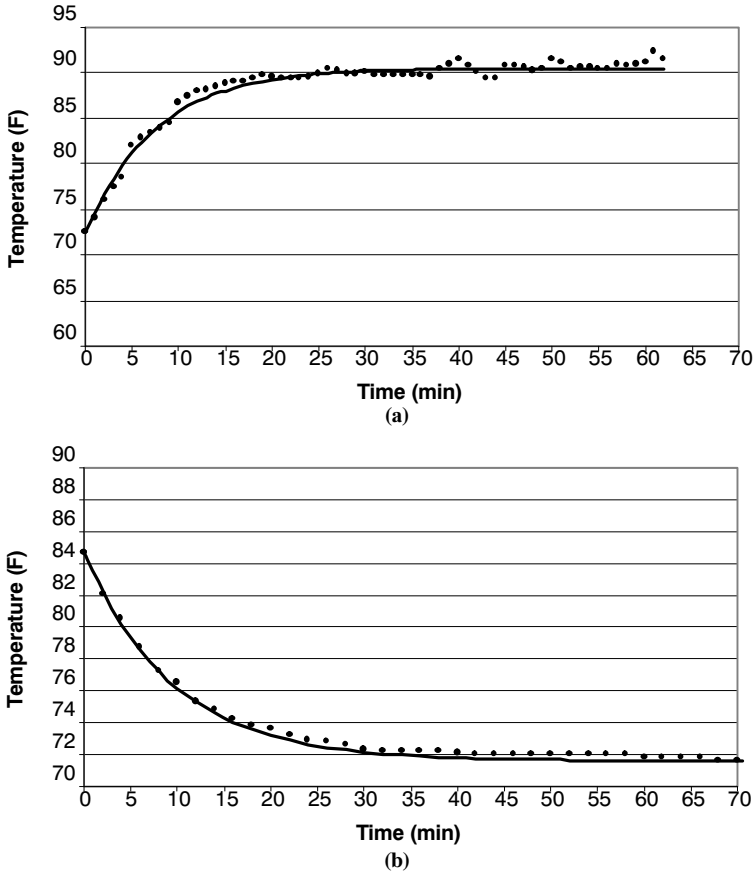

Figure 13. (a) Heating and (b) cooling behavior of the developed IR sensor. Actual (□) IR sensor response compared to first-ordered exponential behavior (-) using experimentally measured time constants of 7.5-min (heating, a) and 9.5-min (cooling, b).

References

Barnard, J. A., and J. N. Bradley. 1985. *Flame and Combustion,* 2nd ed. New York: Chapman and Hall Publishing.

Davis, J. D., R. D. MacDonald, and H. Xin. 2006. Infrared thermography evaluation of commercially available infrared heat lamps. ASABE Paper No. 064152. St. Joseph, Mich.: ASABE.

Hall, C. W. 1962. Theory of infrared drying. *Trans. ASAE* 5(1): 14-16.

Hoff, S. J. 2003. Infrared radiant sensing for controlling IR-based heaters. In *Swine Housings II Proc.* St. Joseph, Mich.: ASAE.

Holman, J. P. 2002. *Heat Transfer,* 9th ed. New York: McGraw-Hill, Inc.

Houszka, H. M., J. S. Strøm, and S. Morsing. 2001. Thermal conditions in covered creep areas for piglets. *Trans. ASAE* 44(6): 1859-1863.

Ibrahim, M., and T. D. Briselden. 2002. High-temperature, non-catalytic, infrared heater. United States Patent Number 6368102.

Kuppenheim, H. F., J. M. Dimitroff, P. M. Melotti, I. C. Graham, and D. W. Swanson. 1956. Spectral reflectance of the skin of Chester White Pigs in the ranges 235.700 mu and 0.707-2.6 μ. *J. Applied Physiol.* 9: 75-78.

Miller, J. L. 1994. *Principles of Infrared Technology: A Practical Guide to the State of the Art.* New York: Van Nostrand Reinhold Publishing.

Modest, M. F. 1993. *Radiative Heat Transfer.* New York: McGraw-Hill, Inc.

Omega Engineering, Inc. 2008. Available at: www.omega.com/literature/transactions/volume1/emissivitya.html. Accessed 8 August 2008.

Raytek, Inc. 2008. Emissivity table for non-metals. Available at: www.raytek.com/Raytek/en-r0/IREducation/EmissivityNonMetals.htm. Accessed 8 September 2008.

Shilton, N., H. Carnahan, J. Forman, S. Fermanian, K. Mallikarjunan, and D. Vaughan. 2002. Modeling of the heat transfer in food products cooked with far infrared radiation. ASAE Paper No. 026044. St. Joseph, Mich.: ASAE.

The Engineering Toolbox. 2008. Emissivity coefficients of some common materials. Available at: www.engineeringtoolbox.com/emissivity-coefficients-d_447.html. Accessed 1 October 2008.

Wheeler, E. F., G. Vasdal, A. Fløe, and K. E. Bøe. 2008. Static space requirements for piglet creep area as influenced by radiant temperature. *Trans. ASABE* 51(1): 271-278.

Zhang, Q., and H. Xin. 2001. Responses of piglets to creep heat type and location in farrowing crate. *Applied Eng. in Agric.* 17(4): 515-519.

Zhou, H., and H. Xin. 2001. Effects of heat lamp output and color on piglets at cool and warm environments. *Applied Eng. in Agric.* 15(4): 327-330.

Nomenclature

A = area, m^2
AOZ = animal occupied zone
AWAT = area weighted average temperature, C
F = shape factor (0-1)
h = convective heat transfer coefficient, W/m^2-K
IR = infrared energy
n = number of shields for an IR receiver
q = heat flux, W/m^2
Q = total heat, W
R = either a specific radius (cm) or auxiliary variable (dimensionless) used in shape factor calculations
T = temperature, K
TC = thermocouple (T-type used)
X = auxiliary variable used in shape factor calculations
y = vertical distance from IR heater to IR sensor, cm
Y = vertical distance from IR heater to floor, cm

Greek Symbols

α = surface absorptivity which depends on source surface temperature (0-1)
ε = surface emissivity which depends on surface temperature of emitter (0-1)
λ = wavelength, μm
η = IR heater efficiency in conversion of combustion energy to a radiating surface temperature (0-1)
σ = Stefan-Boltzmann constant, 5.67×10^{-8} W/m^2-K^4

Subscripts

floor = conditions at the floor of the AOZ
sensor = conditions at the sensor within the IR heating zone
absorbed = absorbed infrared energy
∞ = conditions outside the IR heating zone
t = total
j = index for temperature sensors in the experimental set-up
i = index for discretized rings used in theoretical analysis
h = relative to IR heater
o = outside location
i = inside location
r = pertaining to some radial distance
1,2,3 = pertaining to unique surfaces in an enclosure